

## Microwave and radio frequency spectra of Xe–HF

F. A. Baiocchi, T. A. Dixon, C. H. Joyner, and W. Klemperer

Citation: *The Journal of Chemical Physics* **75**, 2041 (1981); doi: 10.1063/1.442322

View online: <http://dx.doi.org/10.1063/1.442322>

View Table of Contents: <http://scitation.aip.org/content/aip/journal/jcp/75/5?ver=pdfcov>

Published by the AIP Publishing

---

### Articles you may be interested in

[Microwave and radio frequency spectrum of XeHCl](#)

J. Chem. Phys. **70**, 5157 (1979); 10.1063/1.437356

[Spectroscopy at Radio and Microwave Frequencies](#)

Am. J. Phys. **36**, 768 (1968); 10.1119/1.1975139

[Erratum: RadioFrequency and Microwave Spectra of LiBr by the MolecularBeam ElectricResonance Method](#)

J. Chem. Phys. **47**, 2202 (1967); 10.1063/1.1712263

[RadioFrequency and Microwave Spectra of NaF by the MolecularBeam ElectricResonance Method](#)

J. Chem. Phys. **41**, 3540 (1964); 10.1063/1.1725764

[RadioFrequency and Microwave Spectra of LiBr by the MolecularBeam ElectricResonance Method](#)

J. Chem. Phys. **41**, 2368 (1964); 10.1063/1.1726273

---



# Microwave and radio frequency spectra of Xe-HF<sup>a)</sup>

F. A. Baiocchi, T. A. Dixon, C. H. Joyner, and W. Klemperer

Department of Chemistry, Harvard University, Cambridge, Massachusetts 02138  
(Received 27 March 1981; accepted 22 May 1981)

The spectroscopic constants for Xe-HF obtained from molecular beam electric resonance spectroscopy are as follows:

	$B_0$ (MHz)	$D_0$ (MHz)	$eQq_a$ ( $^{131}\text{Xe}$ ) (MHz)	$\mu$ (D)
$^{129}\text{Xe-HF}$	2039.690(4)	0.018 32(19)	...	1.7359(4)
$^{131}\text{Xe-HF}$	2035.563(5)	0.018 19(16)	-8.589(39)	...
$^{132}\text{Xe-HF}$	2033.552(5)	0.018 19(20)	...	...
$^{129}\text{Xe-DF}$	1995.469(5)	0.015 87(16)	...	1.9537(7)
$^{131}\text{Xe-DF}$	1991.268(3)	0.015 77(9)	-10.567(27)	...
$^{132}\text{Xe-DF}$	1989.217(4)	0.015 73(14)	...	...

The structure and weak bond force constants derived from the spectroscopic constants are consistent with data on other noble gas-hydrogen fluoride complexes. It is found that the electric field gradient at the Xe nucleus for a given HF orientation scales with the electric field gradient arising from HF.

## INTRODUCTION

The study of the structural and dynamic properties of the noble gas-hydrogen halide gas phase complexes has been extended to the Xe-HF dimer. This augments the spectroscopic data available for these complexes, and it will be seen that the properties of Xe-HF are consistent with the other noble gas-hydrogen halide complexes. Also, this is the third species for which the perturbation of the electron density of the noble gas atom, as measured by the nuclear quadrupole coupling constant, has been determined. The relevant quantity is  $eQq_a$ , with the nuclear quadrupole moment ( $Q$ ) a fixed property of the  $^{131}\text{Xe}$  nucleus, and the electric field gradient along the "a" inertial axis of the complex ( $-q_a$ ) a variable dependent on the interaction. This constant has already been measured for  $^{83}\text{Kr-HF}$ ,  $^{83}\text{Kr-DF}$ ,  $^{16}\text{O}$  and  $^{131}\text{Xe-H}^{35}\text{Cl}$ .<sup>2</sup> It was concluded that  $q_a$  in those species could be attributed to an induction effect on the polarizable rare gas atom by the hydrogen halide. (This is sometimes referred to as Sternheimer shielding or anti-shielding.)

In this work, the nuclear quadrupole coupling constant is reported for both the hydrogen and deuterium isotopes of  $^{131}\text{Xe-HF}$ . Since the intermolecular potential is independent of isotopic substitution, availability of data for both isotopes makes it possible to sample two different regions of the Xe-HF potential surface, allowing a possible determination of  $q_a$  for the equilibrium structure. Further, the dipole moment for both isotopes is reported. A comparison of these two electrical properties of the molecule is then possible for two average HF orientations.

The Xe-HF system has been studied previously. Scattering studies using crossed beams<sup>3</sup> of Xe and HF have

been used to generate several model potential surfaces characterizing the Xe-HF interaction. Also, spectroscopic studies have been done in which the shifts of HF vibration-rotation lines have been measured in xenon matrices<sup>4,5</sup> and in xenon and hydrogen fluoride gas mixtures.<sup>6,7</sup> In the present work the rotational spectra, unperturbed by collision, of the ground vibrational state of Xe-HF are reported.

## EXPERIMENTAL

The work was done using a molecular beam electric resonance spectrometer. The apparatus and experimental technique used to obtain the rotational spectrum has been described elsewhere.<sup>8</sup> The complex was synthesized by expanding a room temperature mixture of argon, xenon, and hydrogen fluoride in the approximate ratio 100:1.5:0.5 through a 25  $\mu$  diameter nozzle at a stagnation pressure of 3 atm. It was found that Xe-HF production decreased if the HF concentration in the mixture was 1.5%-2%. At these higher concentrations, formation of HF polymers interfered with production of the complex.

Isotopes of Xe-HF were detected mass spectrometrically at the parent ion peak ( $m/e=149-156$ ) and at the  $\text{Xe}^+$  ion peak ( $m/e=129-136$ ). The S/N ratio for Xe-HF transitions was greater at the latter mass peak and so spectroscopy was done while monitoring this mass. Six isotopes were studied. These were  $^{129}\text{Xe}$ ,  $^{131}\text{Xe}$ , and  $^{132}\text{Xe}$  bound to HF and DF. The  $^{129}\text{Xe}$  isotope has a nuclear spin  $I=\frac{1}{2}$ . This nuclear magnetic dipole was found to have no effect on the measured rotational transitions or Stark components, at the level of resolution of the apparatus ( $\sim 20$  kHz linewidths in the microwave region and  $\sim 2$  kHz linewidths in the radio frequency region). The  $^{132}\text{Xe}$  isotope has no nuclear spin.

Rotational constants and  $eQq_a$  ( $^{131}\text{Xe}$ ) were determined from the measured rotational transitions at zero electric

<sup>a)</sup>This research was supported by the National Science Foundation.

field. Dipole moments, the HF nuclear spin-spin coupling constant ( $S_a$ ), and  $eQq_a$  (D) for  $^{129}\text{Xe}$ -HF and  $^{129}\text{Xe}$ -DF were determined from the  $J=1$ ,  $M_J=0 \rightarrow 1$

TABLE I. Measured zero-field transitions.<sup>a</sup>

$^{129}\text{Xe}$ -HF				
$J$	$F$	$J'$	$F'$	$\nu$ (MHz)
0	1	1	2	4 079.316(18)
0	1	1	0	4 079.376(15)
1	2	2	3	8 158.173(17)
1	1	2	2	
3	4	4	5	16 312.828(30)
3	3	4	4	

$^{131}\text{Xe}$ -HF				
$J$	$F_1$	$J'$	$F_1'$	$\nu$ (MHz)
0	3/2	1	1/2	4 073.202(10)
1	1/2	2	1/2	8 141.672(20)
1	5/2	2	7/2	8 141.856(30)
1	3/2	2	1/2	8 145.534(12)
3	9/2	4	9/2	16 277.765(50)
3	3/2	4	5/2	16 279.655(35)
3	5/2	4	5/2	16 281.825(40)
3	7/2	4	5/2	16 282.814(27)

$^{132}\text{Xe}$ -HF				
$J$	$F$	$J'$	$F'$	$\nu$ (MHz)
1	2	2	3	8 133.625(14)
1	1	2	2	
3	4	4	5	16 263.760(25)
3	3	4	4	

$^{129}\text{Xe}$ -DF				
$J$	$F_1$	$J'$	$F_1'$	$\nu$ (MHz)
1	1	2	2	7 981.364(30)
1	2	2	2	7 981.438(15)
3	3	4	3	15 959.597(10)
3	3	4	4	15 959.690(25)
3	4	4	4	15 959.766(15)

$^{131}\text{Xe}$ -DF				
$J$	$F_1$	$J'$	$F_1'$	$\nu$ (MHz)
1	1/2	2	1/2	7 964.566(15)
1	5/2	2	7/2	7 964.798(14)
1	3/2	2	1/2	7 969.322(10)
3	9/2	4	9/2	15 923.541(25)
3	5/2	4	5/2	15 928.524(10)
3	7/2	4	5/2	15 929.756(15)

$^{132}\text{Xe}$ -DF				
$J$	$F_1$	$J'$	$F_1'$	$\nu$ (MHz)
1	1	2	2	7 956.364(25)
1	2	2	2	7 956.432(12)
3	3	4	3	15 909.612(25)
3	3	4	4	15 909.714(25)
3	4	4	4	15 909.784(20)

<sup>a</sup>Reported uncertainties are full width at half-height divided by the S/N ratio.  $F_1 = J+I$ , where  $I$  is the spin of the nucleus causing greatest perturbation of the rotational energy levels.

TABLE II. Measured transitions at nonzero static electric fields (MHz).<sup>a</sup>

$ M_F $	$ M_F $	300.0 V/cm	400.0 V/cm
$^{129}\text{Xe}$ -HF			
$J=1$ , $M_J=0 \rightarrow  M_J =1$			
1	0	4.987(4)	8.904(3)
1	2	5.030(2)	8.946(4)
0	1	5.050(3)	8.968(3)
1	0	5.072(5)	8.989(4)
0	1	5.093(4)	9.010(2)

$^{129}\text{Xe}$ -DF			
$J=1$ , $M_J=0 \rightarrow  M_J =1$			
1/2	1/2	6.431(3)	
1/2	3/2	6.468(8)	
1/2	3/2	6.491(8)	
1/2	1/2	6.505(5)	
1/2	1/2	6.547(6)	
3/2	5/2	6.559(6)	
1/2	3/2	6.576(8)	
1/2	3/2	6.633(6)	
1/2	1/2	6.644(6)	

<sup>a</sup>Reported uncertainties are full width at half-height divided by the S/N ratio.

transition of  $^{129}\text{Xe}$ -HF and  $^{129}\text{Xe}$ -DF at applied homogeneous electric fields. The electric field can be set with a precision of four significant digits.

## RESULTS

The measured transition frequencies are listed in Tables I and II, and Fig. 1 shows a typical microwave line of  $^{131}\text{Xe}$ -HF. Except for the  $J=0 \rightarrow 1$  transition of  $^{129}\text{Xe}$ -HF, no splitting of the rotational transitions of Xe-HF by the HF nuclear spin-spin interaction was observed. Hence, the zero-field data for the hydrogen isotopes is analyzed using the standard energy level expression<sup>9</sup>

$$E = B_F J(J+1) - D_F J^2(J+1)^2 - eQq_a(^{131}\text{Xe}) \frac{3}{2} \frac{C(C+1) - I(I+1)J(J+1)}{2I(2I-1)(2J-1)(2J+3)},$$

with  $C = F(F+1) - I(I+1) - J(J+1)$ . The unsplit line

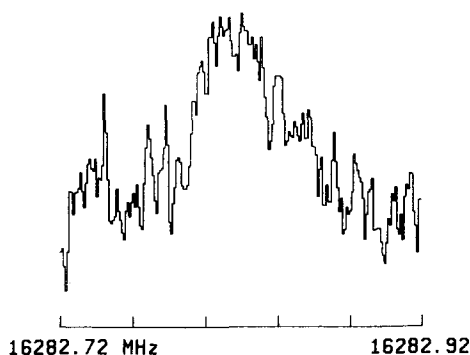


FIG. 1. The  $F_1 = \frac{7}{2} \rightarrow \frac{5}{2}$  hyperfine component of the  $J=3 \rightarrow 4$  transition of  $^{131}\text{Xe}$ -HF. This is the average of eight scans at a time constant of 3 sec and a resolution of 1 kHz/channel.

position of the  $J=0 \rightarrow 1$  transition of  $^{129}\text{Xe-HF}$  for use in this analysis is calculated with the value of  $S$  (the HF spin-spin coupling constant) as determined from the rf measurements.

For the Xe-DF isotopes, splittings in the rotational transitions due to the deuterium nuclear quadrupole and DF spin-spin interactions are observed. The  $^{129}\text{Xe-DF}$  and  $^{132}\text{Xe-DF}$  data are combined and, using the above energy level expression, fit to five parameters:  $B_0$  and  $D_0$  for both isotopes and  $eQq_a(\text{D})$ . In the case of  $^{131}\text{Xe-DF}$ , calculations of line strengths showed that the most intense lines would be those that were basically unsplit by the deuterium nuclear quadrupole interaction. Hence zero-field transitions of  $^{131}\text{Xe-DF}$  were measured at microwave power levels sufficiently low to justify the neglect of hyperfine splitting due to deuterium. This data is then analyzed using the energy level expression given above. The rotational constants  $B_0$ , distortion constants  $D_0$ , and quadrupole coupling constants obtained from the zero-field data are reported in Table III.

The  $J=1$ ,  $M_J=0 \rightarrow 1$  transition was observed in  $^{129}\text{Xe-HF}$  at two electric field settings and in  $^{129}\text{Xe-DF}$  at one field setting. The spectrum obtained for  $^{129}\text{Xe-HF}$  at an electric field strength of 300 V/cm is shown in Fig. 2. The signal-to-noise ratio is poor for the rf transitions because at the low focusing fields required, the fraction of mass spectrometer signal due to  $^{129}\text{Xe-HF}$  is small compared to the large  $^{129}\text{Xe}$  background at  $m/e$  129. Except for the magnitude of the splitting, the hyperfine patterns obtained for  $^{129}\text{Xe-HF}$  and  $^{129}\text{Xe-DF}$  are nearly identical to those obtained for the same transitions in Ar-HF and Ar-DF, and are analyzed in the same manner<sup>10(a)</sup> to yield values for the dipole moment ( $\mu_a$ ),  $S_a$ , and  $eQq_a(\text{D})$ .

It is assumed that  $eQq_a(\text{D})$  and  $S_a$  can be expressed as projections onto the  $a$  axis of the relevant coupling constants for free HF:

$$eQq_a(\text{D}) = \langle P_2(\cos\theta) \rangle eQq_0(\text{D}),$$

$$S_a = \langle P_2(\cos\theta) \rangle S_0.$$

TABLE III. Spectroscopic constants of Xe-HF.<sup>a</sup>

Zero-field results				
	$B_0$ (MHz)	$D_0$ (MHz)	$eQq_a(^{131}\text{Xe})$ (MHz)	$eQq_a(\text{D})$ (MHz)
$^{129}\text{Xe-HF}$	2039.690(4)	0.018 32(19)		
$^{131}\text{Xe-HF}$	2035.563(5)	0.018 19(16)	- 8.589(39)	
$^{132}\text{Xe-HF}$	2033.552	0.018 19		
$^{129}\text{Xe-DF}$	1995.469(5)	0.015 87(16)		0.223(19)
$^{131}\text{Xe-DF}$	1991.268(3)	0.015 77(9)	-10.567(27)	
$^{132}\text{Xe-DF}$	1989.217(4)	0.015 73(14)		0.223(19)
Non-zero-field results				
	$\mu$ (D)	$P_2(\cos\theta)$	$eQq_a(\text{D})$ (MHz)	$S_a$ (MHz)
$^{129}\text{Xe-HF}$	1.7359(4)	0.493(6)		0.0707
$^{129}\text{Xe-DF}$	1.9537(7)	0.638(1)	0.226	0.0141

<sup>a</sup>Reported uncertainties are derived from least-squares analysis and adjusted to 97% confidence limits.

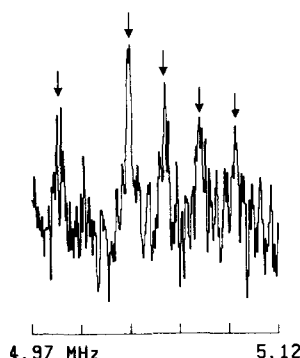


FIG. 2.  $J=1$ ,  $\Delta M_J=1$  Stark spectra at 300 V/cm. This is the average of eight scans at a time constant of 3 sec and a resolution of 0.5 kHz/channel.

$eQq_0(\text{D})$  and  $S_0$  are the constants of HF, and  $\theta$  is the angle made by the HF submolecule with the principal axis ( $P_2$  is the second Legendre polynomial). The validity of this assumption is borne out by results<sup>10</sup> on Ar-DF. In that complex, the rf data could be fit to  $eQq_a(\text{D})$  and  $S_a$  independently, and the projection angles obtained from each agreed to within the experimental uncertainty. This indicates a minimum perturbation of HF properties by the noble gas atom. The  $J=1$ ,  $M_J=0 \rightarrow 1$  transition is then fit to two parameters,  $\mu$  and  $P_2(\cos\theta)$ , for both isotopes. The results of this fit are given in Table III. Included in this table are values of  $S_a$  and  $eQq_a(\text{D})$  derived using the above expressions and the coupling constants<sup>11</sup> of HF.

The average structure of Xe-HF can now be estimated from the spectroscopic constants. Two structural parameters are defined:  $r_{\text{c.m.}}$ , the distance between xenon and the diatom center of mass, and  $\gamma$ , the angle made by HF with the line defining  $r_{\text{c.m.}}$ . (The HF bond length is assumed to be the same as in the free molecule.) These two parameters are adjusted to reproduce  $B_0$  and  $\theta$ . The resulting values of  $r_{\text{c.m.}}$  for the three hydrogen isotopes are identical to five digits, and the three deuterium isotopes behave similarly. Hence only two values of  $r_{\text{c.m.}}$  are reported. Two values of  $\gamma$  are consistent with the projection angle  $\theta$  for a given isotope, with the acute value corresponding to a structure in which the hydrogen atom points towards Xe. Isotopic substitution of the hydrogen atom allows unambiguous determination of the correct angle. We find that for the acute choice of angle, the Xe-F distance decreases by 0.004 Å on deuterium substitution, whereas this distance decreases by 0.082 Å for the obtuse choice. The decrease for the obtuse angle is unreasonably large when compared to the observed decrease in the Xe-F distance between  $^{129}\text{Xe-HF}$  and  $^{132}\text{Xe-HF}$ , which is 0.000 07 Å. Using a reduced mass given by  $M_s = m_{\text{Xe}}m_{\text{HF}}/(m_{\text{Xe}} + m_{\text{HF}})$ , it is found that  $M_s$  changes by 0.3% on substitution of  $^{132}\text{Xe}$  for  $^{129}\text{Xe}$ .  $M_s$  changes by 4% on deuterium substitution, predicting a decrease of  $\sim 0.001$  Å. Hence the acute angle is the correct choice. Table IV summarizes the values of  $r_{\text{c.m.}}$ ,  $\gamma$ , and  $\theta$ .

Some notion of the degree of nonrigidity of the complex can be had by relating  $D_0$  and  $\theta$  to force constants and vibrational frequencies for the stretch and bend of the weak bond. This is done by assuming that the vibrational motions can be approximated by a harmonic oscillator model. The distortion constant can then be re-

TABLE IV. Structural and dynamic parameters of Xe-HF.

	<sup>129</sup> Xe-HF	<sup>129</sup> Xe-DF
$r_{\text{c.m.}}$ (Å)	3.7772	3.7339
$r_{\text{Xe-F}}$ (Å)	3.8152	3.8111
$\theta$	35.55	29.4
$\gamma$	35.7	29.55
$k_s$ (mdyn/Å)	0.021	0.024
$\nu_s$ (cm <sup>-1</sup> )	45	47
$k_b$ (mdyne Å)	0.005	0.006
$\nu_b$ (cm <sup>-1</sup> )	100	80

lated to the stretching force constant (in the diatomic approximation) by

$$k_s = \frac{16\pi^2 M_s B_0^3}{D_0}$$

The bending force constant is given by

$$k_b = \frac{\hbar^2}{M_b \langle \gamma^2 \rangle^2}$$

Two assumptions are made in the use of this relation: first, that  $\langle \gamma^2 \rangle$  can be approximated by an angle obtained from  $\langle \cos^2 \theta \rangle$  and second, that  $M_b$ , the bending reduced mass, can be approximated by the moment of inertia of the diatom. Keeping in mind these assumptions, the constants describing the internal dynamics are tabulated in Table IV for the hydrogen and deuterium isotopes of <sup>129</sup>Xe-HF. Nearly identical force constants are obtained for the other xenon isotopes.

The equilibrium structure is expected to be linear. The Xe-H bond length for such a structure ( $r_e$ ) is estimated to be approximately 2.89 Å. Comparison to the sum of the van der Waals radii of xenon and hydrogen (3.28 Å) indicates significant charge cloud interpenetration. If the equilibrium structure is truly linear, the following relation should hold:

$$\frac{\gamma_{\text{Xe-DF}}}{\gamma_{\text{Xe-HF}}} = \sqrt{\frac{M_b^{\text{HF}}}{M_b^{\text{DF}}}}$$

The assumption implicit in the use of this expression is that the angle  $\gamma$  is a good measure of the amplitude of the bending vibration. Using  $\gamma_{\text{Xe-HF}} = 35.7^\circ$ , this relation predicts  $\gamma_{\text{Xe-DF}}$  to be  $30.4^\circ$  as opposed to the measured  $29.6^\circ$ . Given the approximations involved, this fairly close agreement is taken as support for the assumed linear equilibrium structure.

Dipole moments for the hydrogen and deuterium isotopes of Xe-HF indicate a certain amount of charge distortion of the subspecies. In particular, when the projection of the hydrogen fluoride dipole moment ( $\mu_{\text{proj}} = \mu_{\text{HF}} \cos \theta$ ) is subtracted from the measured moment, a dipole moment enhancement of 0.25 and 0.37 D is found for <sup>129</sup>Xe-HF and <sup>129</sup>Xe-DF, respectively. Assuming that the dipole moment of the complex results from projection of the HF dipole moment plus simple induction effects, we can relate  $\mu_a$  to the properties of the subspecies as follows<sup>12</sup>:

$$\mu_a = \langle P_1(\cos \theta) \rangle \left[ \mu_{\text{HF}} + \frac{2\mu_{\text{HF}} \alpha_{\text{Xe}}}{r_{\text{c.m.}}^3} K_1 K_2 \right] + \langle P_2(\cos \theta) \rangle \left[ \frac{3\Theta_{\text{HF}} \alpha_{\text{Xe}}}{r_{\text{c.m.}}^4} K_1 K_2 \right],$$

where

$$K_1 = \left( 1 + \frac{2\alpha_{\text{HF}}}{r_{\text{c.m.}}^3} \right) \text{ and } K_2 = \left( 1 + \frac{4\alpha_{\text{Xe}} \alpha_{\text{HF}}}{r_{\text{c.m.}}^6 - 4\alpha_{\text{Xe}} \alpha_{\text{HF}}} \right).$$

This expression, along with the appropriate constants from Tables III and V, can be used to calculate  $\langle P_1(\cos \theta) \rangle$ , and we find  $\langle P_1(\cos \theta) \rangle = 0.789$  for <sup>129</sup>Xe-HF and 0.882 for <sup>129</sup>Xe-DF. The expression given above represents the first two terms of an infinite series, but inclusion of the next term (the octupole term) lowers  $\langle P_1(\cos \theta) \rangle$  by only 0.5%. If this electrostatic model is correct, the dipole moment for the equilibrium structure can be estimated by putting  $P_1(\cos \theta) = P_2(\cos \theta) = 1$ . This calculation yields an equilibrium dipole moment of 2.3 D.

The principal component of the electric field gradient tensor at the xenon nucleus is another molecular property that can be determined from the spectroscopic constants. The constant  $eQq_a(^{131}\text{Xe})$  given in Table III can easily be related<sup>13</sup> to  $q_a$ . We obtain  $9.87 \times 10^{14}$  SC/cm<sup>3</sup> for <sup>131</sup>Xe-HF and  $12.15 \times 10^{14}$  SC/cm<sup>3</sup> for <sup>131</sup>Xe-DF.  $q_a$  is defined<sup>9</sup> as  $d^2V/da^2$ , hence the field gradient is simply given by  $(\nabla E)_{aa} = -q_a$ . Since values of the field gradient for two different orientations of the submolecule are available, it should be possible to estimate a value for the equilibrium structure.

The field gradient at the xenon nucleus due to HF can be expressed as a series expansion<sup>14</sup> in terms of the HF multipole moments:

$$(\nabla E)_{aa}^{\text{HF}} = - \frac{6\mu \langle P_1(\cos \theta) \rangle}{r_{\text{c.m.}}^4} - \frac{12\Theta \langle P_2(\cos \theta) \rangle}{r_{\text{c.m.}}^5} - \frac{20\Omega \langle P_3(\cos \theta) \rangle}{r_{\text{c.m.}}^6} - \dots$$

The first three terms of this expansion are evaluated using the appropriate constants from Tables IV and V. Values of  $P_3(\cos \theta)$  are estimated using  $\theta$  obtained from  $\langle P_2(\cos \theta) \rangle$ . The error involved in estimation of  $P_3(\cos \theta)$ ,

TABLE V. Constants of Xe and HF.

	HF	DF	Xe
$\alpha$ (Å <sup>3</sup> ) <sup>a</sup>	0.915	0.937	4.016
$\mu$ (D) <sup>b</sup>	1.8265	1.8188	...
$\Theta$ (D Å) <sup>c</sup>	2.36	2.21	...
$\Omega$ (D Å <sup>2</sup> ) <sup>d</sup>	1.9	1.8	...

<sup>a</sup>J. S. Muentzer, J. Chem. Phys. 56, 5409 (1972). The value of  $\alpha$  reported is the principal axis component of the polarizability tensor.

<sup>b</sup>Reference 11.

<sup>c</sup>F. H. deLeeuw and A. Dymanus, J. Mol. Spectrosc. 48, 427 (1973). The value for DF was obtained by adjusting the HF value for the shift in the center of mass.

<sup>d</sup>R. D. Amos, Mol. Phys. 35, 1765 (1978).

however, should not significantly affect the calculation since the third term contributes only  $\sim 4\%$  to the sum of the three. The first term contributes  $\sim 66\%$  to the total and the second term contributes  $\sim 30\%$ . The field gradient is calculated to be  $-6.22 \times 10^{12}$  SC/cm<sup>3</sup> for <sup>131</sup>Xe-HF and  $-7.75 \times 10^{12}$  SC/cm<sup>3</sup> for <sup>131</sup>Xe-DF. This only accounts for 0.6% of the measured field gradient. However, it is expected that the main contribution to the field gradient arises from distortion of the xenon electron distribution by the diatom. If it is assumed that the actual field gradient at the xenon nucleus is proportional to  $(\nabla E)_{aa}^{HF}$ , i.e.,  $(\nabla E)_{aa} = c(\nabla E)_{aa}^{HF}$ , then  $c$  is found to be 159 and 157 for the hydrogen and deuterium isotopes, respectively. The agreement between the isotopes seems to support the assumption that the field gradient at the Xe nucleus scales with the field gradient due to a given orientation of the diatom. The field gradient for the equilibrium configuration is then calculated using the expression  $(\nabla E)_e = c(\nabla E)_{aa}^{HF}$ , where  $(\nabla E)_{aa}^{HF}$  is evaluated for the linear structure by setting  $P_1 = P_2 = P_3 = 1$ . This gives  $(\nabla E)_e = -16 \times 10^{14}$  SC/cm<sup>3</sup>, or  $(eQq)_e = -14$  MHz.

## DISCUSSION

The structure and force field parameters of Xe-HF are consistent with similarly derived parameters in the complexes Ar-HF<sup>10</sup> and Kr-HF.<sup>1</sup> The estimated pseudo-equilibrium noble gas-hydrogen bond lengths increase as expected with increasing size of the noble gas atom ( $r_e = 2.62$ ,  $2.72$ , and  $2.89$  Å for the Ar, Kr, and Xe complexes, respectively). It is interesting to note that the differences in  $r_e$  between the complexes mimic the differences in van der Waals radii between the atoms ( $r_{vdw} = 1.92$ ,  $1.98$ , and  $2.18$  Å for Ar, Kr, and Xe). The force constants of the three species also follow a predictable trend. Comparison of the stretching force constants shows that the strongest interaction occurs in Xe-HF [ $k_s$ (mdyn/Å) is 0.014, 0.018, and 0.021 for the Ar, Kr, and Xe complexes]. Available data on the bending force constant shows similar behavior ( $k_b$ (mdyne·Å) is 0.003, 0.004, and 0.005 for the Ar, Kr, and Xe com-

plexes). In a simple-minded view of the interaction, we would expect the strongest bond to form between hydrogen fluoride and the most polarizable of the three atoms, and this is what happens (the polarizabilities<sup>15</sup> are 1.63, 2.46, and 4.02 Å<sup>3</sup> for Ar, Kr, and Xe).

Becker *et al.*<sup>3</sup> have obtained beam scattering data for the Xe and HF system, and have analyzed this data in terms of an isotropic potential  $V(R)$  as well as four different anisotropic potentials  $V(R, \gamma)$ .  $R$  and  $\gamma$  defined in their work are the same as  $r_{c.m.}$  and  $\gamma$  defined in this work.  $R_m$ , the value of  $R$  at the minimum, was calculated for each model potential. They obtained  $R_m = 3.77$  Å from  $V(R)$  and values ranging from  $R_m = 3.73$  to 3.88 Å from the four potentials  $V(R, \gamma)$  (at  $\gamma = 0^\circ$ ). The value obtained in this work ( $r_{c.m.} = 3.7772$  Å), although not strictly comparable to  $R_m$ , shows satisfying agreement with the scattering results. Values of  $k_s$  and  $k_b$  can also be extracted from the four model potentials  $V(R, \gamma)$  and compared with the present results. Potential models a and c of Ref. 3 give negative values for the bending force constants and hence are not included in the comparison. Unfortunately, the second derivative with respect to  $R$  is discontinuous at  $R = R_m$ ; hence we must average two values of  $k_s$ . We obtain  $k_s = 0.023$  mdyn/Å,  $k_b = 0.002$  mdyn Å from model b, and  $k_s = 0.020$ ,  $k_b = 0.004$  from model d. These agree surprisingly well with the measured values, which are,  $k_s = 0.021$  mdyn/Å,  $k_b = 0.005$  mdyn Å. This agreement is probably fortuitous, considering the aforementioned discontinuity in  $d^2V/dR^2$  at  $R_m$ .

An idea of the relative strength of the Xe-HF interaction can also be had by comparison of the electric field gradient at the xenon nucleus to the field gradients obtained for the similar molecules Xe-HCl<sup>2</sup> and Kr-HF.<sup>1</sup> Since the molecules have different average structures, comparison of  $(\nabla E)_e$  would be preferred. The field gradient at xenon appears to be proportional to the field gradient due to HF. We assume a similar behavior for the other species and estimate  $(\nabla E)_e$  for them.<sup>16</sup> In Table VI, the measured values of  $(\nabla E)_{aa}$  are listed, as

TABLE VI. Comparison of field gradients in some Xe and Kr species.

	$eQq_a$ (MHz)	$(\nabla E)_{aa}$ ( $10^{14}$ SC/cm <sup>3</sup> )	$(eQq)_e$ (MHz)	$(\nabla E)_e$ ( $10^{14}$ SC/cm <sup>3</sup> )
<sup>131</sup> Xe-HF	-8.589	-9.87	-14	-16
<sup>131</sup> Xe-DF	-10.567	-12.15	-14	-16
<sup>83</sup> Kr-HF <sup>a</sup>	10.23	-5.23	20	-10
<sup>83</sup> Kr-DF <sup>a</sup>	13.83	-7.07	20	-10
<sup>131</sup> Xe-HCl <sup>b</sup>	-4.9	-5.6	-9	-10
<sup>131</sup> Xe( <sup>3</sup> P <sub>2</sub> ) <sup>c</sup>	-505	-581		
<sup>83</sup> Kr( <sup>3</sup> P <sub>2</sub> ) <sup>d</sup>	904.4	-462		
<sup>129</sup> Xe*F <sub>2</sub> <sup>e</sup>	-2490	-838		
<sup>129</sup> Xe*Cl <sub>2</sub> <sup>e</sup>	-1800	-605		

<sup>a</sup>Reference 1.

<sup>b</sup>Reference 2.

<sup>c</sup>Reference 17.

<sup>d</sup>Reference 18.

<sup>e</sup>G. J. Perlow, *Chemical Applications of Mössbauer Spectroscopy*, edited by V. I. Goldanskii and P. H. Herber (Academic, New York, 1968).  $Q$  of <sup>129</sup>Xe\* =  $-0.41 \times 10^{-24}$  cm<sup>2</sup>.

well as the estimated values of  $(\nabla E)_e$  for the three van der Waals species. The trend established by  $(\nabla E)_e$  is the expected one and correlates with the trend in bond strengths. The larger field gradient observed for Xe-HF compared to Xe-HCl is consistent with the larger dipole moment of HF. Further, the larger field gradient of Xe-HF compared to Kr-HF is attributable to the greater ease with which the Xe atom is polarized by an external charge distribution.

Next, the possibility of charge transfer between Xe and HF is considered. As pointed out above, charge overlap between the two species is indicated since the weak bond length is smaller than the sum of the van der Waals radii. This does not necessarily mean that charge transfer occurs. An idea of the expected magnitude of charge transfer may be had by comparison of the equilibrium field gradient for the van der Waals species to values of the field gradient for the  $^3P_2$  state of the free atom. Atomic beam studies<sup>17,18</sup> have yielded quadrupole coupling constants ( $B$ ) for  $^{131}\text{Xe}(^3P_2)$  and  $^{83}\text{Kr}(^3P_2)$ . The resulting field gradients<sup>19</sup> are listed in Table VI. The  $^3P_2$  state corresponds to the valence electronic configuration  $np^5(n+1)s^1$ , and hence these are the field gradients arising from transfer of one  $p_z$  electron out of the valence  $p$  shell. The ratio of  $(\nabla E)_e$  to the appropriate atomic field gradient is 0.028 for  $^{131}\text{Xe-HF}$ , 0.017 for  $^{131}\text{Xe-HCl}$ , and 0.022 for  $^{83}\text{Kr-HF}$ . Hence, only 2% to 3% of the effect on the field gradient due to removal of one valence  $p_z$  electron is observed in the van der Waals species. For further comparison we include in Table VI values of the field gradient at the xenon nucleus in the nuclear excited states of  $^{129}\text{XeF}_2$  and  $^{129}\text{XeCl}_2$  as obtained from Mössbauer spectroscopy. Again, the field gradients in the xenon van der Waals species are only 2% to 3% of the field gradients observed in the stable xenon compounds indicating little, if any, charge transfer.

If the observed field gradient is attributed solely to an induction effect (i.e., Sternheimer shielding), then the constant  $c$  (as defined in the relation  $(\nabla E)_{aa} = c(\nabla E)_{aa}^{\text{HF}}$ ) is simply  $1 - \gamma_{\text{Xe}}$ , where  $\gamma$  is the shielding constant. The Xe-HF results predict  $\gamma_{\text{Xe}} = -157$ . A similar analysis of the Xe-HCl and Kr-HF results predicts  $\gamma_{\text{Xe}} = -159$  and  $\gamma_{\text{Kr}} = -75$ . These experimentally derived values can be compared to some calculated values of the shielding constant  $\gamma_{\text{Xe}}$  (Ref. 2) = -138,  $\gamma_{\text{Xe}}$  (Ref. 21) = -177 and  $\gamma_{\text{Kr}}$  (Ref. 20) = -41,  $\gamma_{\text{Kr}}$  (Ref. 2) = -68. The difference in the two numbers available for each atom point out the rather large uncertainties involved in the calculation of  $\gamma$ . Given these uncertainties, the "experimentally" predicted shielding constants are the same as the calculated ones. It is probable that Sternheimer shielding accounts for most, if not all, of the observed field gradients in these molecules, but given the small size of the effect, the errors involved in evaluation of  $\gamma$ , and the uncertainty in the use of the simple electrostatic model to estimate  $c$ , the fraction ascribable to Sternheimer shielding cannot be conclusively determined. Alternatively, the fraction due to charge transfer is also undetermined.

It is interesting that the proportionality constant  $c$  calculated for Xe-HF is practically identical to the value

calculated for Xe-HCl. This indicates that  $c$  is a property only of the noble gas atom, and it lends further support to the use of the electrostatic model to calculate properties of the electric charge distribution. The fact that this model seems to work so well is surprising, and perhaps somewhat misleading, considering the short bond length between the noble gas atom and the hydrogen halide. The electrostatic model is an approximation which should work well when the charge distributions are well separated. In these species there is significant charge overlap and the model is expected to be a poor approximation. Nevertheless, the available evidence from these studies suggests that an electrostatic model can be used successfully to calculate the properties of the electric charge distribution of weakly bound noble gas complexes. Experiments to determine  $eQq_a(^{131}\text{Xe})$  in other Xe van der Waals species are being planned to further test the model.

- <sup>1</sup>(a) E. J. Campbell, M. R. Keenan, L. W. Buxton, T. J. Balle, P. D. Soper, A. C. Legon, and W. H. Flygare, *Chem. Phys. Lett.* **70**, 420 (1980); (b) L. W. Buxton, E. J. Campbell, M. R. Keenan, T. J. Balle, and W. H. Flygare, *Chem. Phys.* **54**, 173 (1981).
- <sup>2</sup>M. R. Keenan, L. W. Buxton, E. J. Campbell, T. J. Balle, and W. H. Flygare, *J. Chem. Phys.* **73**, 3523 (1980).
- <sup>3</sup>C. H. Becker, P. W. Tiedemann, J. J. Valentini, Y. T. Lee, and R. B. Walker, *J. Chem. Phys.* **71**, 481 (1979).
- <sup>4</sup>M. G. Mason, W. G. Von Holle, and D. W. Robinson, *J. Chem. Phys.* **54**, 3491 (1971).
- <sup>5</sup>H. Friedmann and S. Kimel, *J. Chem. Phys.* **43**, 3925 (1965).
- <sup>6</sup>J. Jarecki and R. M. Herman, *J. Quantum Spectrosc. Radiat. Transfer* **15**, 707 (1975).
- <sup>7</sup>J. Jarecki, *J. Chem. Phys.* **65**, 5318 (1977).
- <sup>8</sup>T. R. Dyke, G. R. Tomasevich, and W. Klemperer, *J. Chem. Phys.* **57**, 2277 (1972).
- <sup>9</sup>C. H. Townes and A. L. Schawlow, *Microwave Spectroscopy* (Dover, New York, 1975), Chap. 6.
- <sup>10</sup>(a) T. A. Dixon, C. H. Joyner, F. A. Baiocchi, and W. Klemperer, *J. Chem. Phys.* **74**, 6539 (1981); (b) M. R. Keenan, L. W. Buxton, E. J. Campbell, A. C. Legon, and W. H. Flygare, *ibid.* **74**, 2133 (1981).
- <sup>11</sup>J. S. Muentner and W. Klemperer, *J. Chem. Phys.* **52**, 6033 (1970).
- <sup>12</sup>S. E. Novick, S. J. Harris, K. C. Janda, and W. Klemperer, *Can. J. Phys.* **53**, 2007 (1975).
- <sup>13</sup> $q_a = (\text{coupling constant}) \times h/eQ$ , where  $Q$  is  $-0.12 \times 10^{-24} \text{ cm}^2$  for  $^{131}\text{Xe}$  (see Ref. 17). Note that  $q_a$  (cgs units) =  $(3.3357 \times 10^{-7}) q_a$  (SI units).
- <sup>14</sup>A. D. Buckingham, *Adv. Chem. Phys.* **12**, 107 (1967).
- <sup>15</sup>P. J. Leonard, *At. Data Nucl. Data Tables* **14**, 21 (1974).
- <sup>16</sup>A dipole moment measurement is available for  $^{131}\text{Xe-HCl}$  [see K. V. Chance, K. H. Bowen, J. S. Winn, and W. Klemperer, *J. Chem. Phys.* **70**, 5157 (1979)], and this was used to calculate  $\langle P_1(\cos\theta) \rangle$  for it.  $\mu$ ,  $\Theta$ ,  $r_{\text{cm}}$ , and  $\langle P_2(\cos\theta) \rangle$  for  $^{131}\text{Xe-HCl}$  were obtained from Ref. 2.  $\Omega$  for HCl was obtained from J. H. Williams and R. D. Amos, *Chem. Phys. Lett.* **70**, 162 (1980).  $r_{\text{cm}}$  and  $\langle P_2(\cos\theta) \rangle$  for  $^{83}\text{Kr-HF}$  were obtained from Ref. 1.
- <sup>17</sup>W. L. Faust and M. N. McDermott, *Phys. Rev.* **123**, 198 (1961).
- <sup>18</sup>W. L. Faust and L. Y. Chow Chiu, *Phys. Rev.* **129**, 1214 (1963).
- <sup>19</sup> $eQq_a = -2B$ .  $Q$  for  $^{83}\text{Kr}$  was obtained from Ref. 18.
- <sup>20</sup>G. Burns and E. G. Wikner, *Phys. Rev.* **121**, 155 (1961).
- <sup>21</sup>F. D. Feiock and W. R. Johnson, *Phys. Rev.* **187**, 39 (1969).